American Mineralogist, Volume 80, pages 1261–1268, 1995

Experimental study of the solid solution between monazite-(La) and $(Ca_{0.5}U_{0.5})PO_4$ at 780 °C and 200 MPa

RENAUD PODOR, MICHEL CUNEY, CHINH NGUYEN TRUNG
CREGU, GdR CNRS-CREGU No. 77, BP 23, 54506 Vandœuvre-Les-Nancy Cedex, France

ABSTRACT

The behavior of Ca and U in the system CaO-UO_2-La_2O_3-H_3PO_4 has been experimentally investigated at 780 °C and 200 MPa and at f_{O_2} conditions fixed by the Ni + NiO buffer. The results obtained indicate that a complete solid solution was formed between $LaPO_4$ and $(Ca_{0.5}U_{0.5})PO_4$. The coupled substitution of two atoms of La^{3+} by U^{4+} + Ca^{2+} is represented by the equation $LaPO_4 + xU^{4+} + xCa^{2+} = (La_{1-2x}U_xCa_x)PO_4 + 2xLa^{3+}$ with the mole fraction x varying from 0 to 0.5. The cell parameters of the solid solution $(La_{1-2x}U_xCa_x)PO_4$ decrease linearly with decreasing amounts of La^{3+}. This is a result of the smaller ionic radii of U^{4+} and Ca^{2+} (1.05 and 1.18 Å, respectively) compared with that of La^{3+} (1.216 Å). The end-member $(Ca_{0.5}U_{0.5})PO_4$ was hydrothermally synthesized for the first time in the system CaO-UO_2-H_3PO_4 under similar experimental conditions. The data obtained show that there is no crystal-chemical limitation to U substitution in monazite crystals at temperature and pressure conditions corresponding to those of granitic magma crystallization, provided that Ca is available.

INTRODUCTION

Monazite is a crystalline mixed-lanthanide orthophosphate [(La,Ce,Nd,Th,Ca)PO_4] of varying composition, which was proposed in the late 1970s as a primary host for the long-term storage of radionuclides. Monazite may contain as much as 31.5 wt% ThO_2 (Overstreet, 1967) and 15.64 wt% UO_2 (Gramaccioli and Segalstad, 1978). The extent of the solid solution is not known, however, and the substitution mechanisms have been deduced only from analytical work on monazite. Large U and Th substitutions must involve coupled substitution of other cations to maintain the charge balance. Two mechanisms were suggested for the substitution of REE^{3+} (rare earth element) by U^{4+}: (1) replacement of two REE^{3+} by Ca^{2+} and U^{4+} according to the equation

$$Ca^{2+} + U^{4+} \rightleftharpoons 2REE^{3+} \quad (1)$$

and (2) substitution of one REE^{3+} by one U^{4+} coupled with a P^{5+} for Si^{4+} substitution leading to the $USiO_4$ (cofinite) end-member according to the equation

$$Si^{4+} + U^{4+} \rightleftharpoons REE^{3+} + P^{5+}. \quad (2)$$

Representative monazite and cheralite analyses reported in the (REE,Ca)(P,Si)O_4-Th(P,Si)O_4-U(P,Si)O_4 diagram show two separate fields of composition (Gramaccioli and Segalstad, 1978). One is close to the monazite composition, and the other is close to the cheralite composition. There seems to be a gap in the U and Th content between minerals with the monazite structure. The present work attempts to determine whether this gap is a result of partial miscibility between the end-members or rather of a limited variation in the conditions of formation. We also report the first systematic data on the crystal structure of monazite containing U.

Syntheses of $LaPO_4$ have been realized by hydrothermal reaction (Anthony, 1957; Montel et al., 1989) and by oxide calcination (Radominski, 1875; Mooney, 1948; Karkhanavala, 1956). However, syntheses of monazite containing U and Th have been performed only by dry techniques: either by the flux fusion method (Anthony, 1965) or by the calcination, pelletization, and crystallization-sintering process (McCarthy et al., 1978; Pepin et al., 1981). Muto et al. (1959) obtained the product $(Ca_{0.5}U_{0.5})PO_4$ by heating synthetic ningyoite $(Ca_{0.5}U_{0.5})PO_4 \cdot 1.5H_2O$ at 900 °C under Ar atmosphere. Pepin et al. (1981) synthesized $(Ca_{0.5}U_{0.5})PO_4$ by a dry method.

The aim of the present study is to determine experimentally the nature of the substitution of La^{3+} by U^{4+} + Ca^{2+} in $LaPO_4$ in the system CaO-UO_2-$LaPO_4$-H_3PO_4 at 780 °C and 200 MPa and at f_{O_2} conditions fixed by the Ni + NiO buffer. The crystal structure of $(La_{1-2x}U_xCa_x)PO_4$ compounds with mole fraction x ranging from 0 to 0.5 was systematically determined. Similarly, the end-member $(Ca_{0.5}U_{0.5})PO_4$ was hydrothermally synthesized for the first time, and its crystallographic characteristics were determined.

MATERIALS AND METHODS

Starting materials and sample preparation

The method used in the present work is similar to that of Anthony (1957). A gel of $La(OH)_3$ was precipitated by the addition of NH_4OH to an aqueous solution of lanthanum chloride. The precipitate was filtered, washed with distilled water, and heated at 600 °C for 30 min. Various amounts of $UO_{2.12}$ and CaO were mixed with the $La(OH)_3$

0003–004X/95/1112–1261$02.00

TABLE 1. Experimental conditions and compositions of initial mixtures and final products

Expt.	Days	Initial mixture	Aqueous phase	P_2O_5 (wt%)
P145	14	78% UO_2-22% CaO	H_3PO_4 = 30 *m*	30.11 ± 0.46
P146	1	60% $La(OH)_3$-32% UO_2-8% CaO	H_3PO_4 = 30 *m*	30.18 ± 0.45
P147	3	60% $La(OH)_3$-32% UO_2-8% CaO	H_3PO_4 = 30 *m*	29.74 ± 0.57
P148	6	60% $La(OH)_3$-32% UO_2-8% CaO	H_3PO_4 = 30 *m*	28.73 ± 0.78
P149	42	60% $La(OH)_3$-32% UO_2-8% CaO	H_3PO_4 = 30 *m*	29.19 ± 0.64
P150	52	60% $La(OH)_3$-32% UO_2-8% CaO	H_3PO_4 = 30 *m*	29.30 ± 0.61
P151	20	60% $La(OH)_3$-32% UO_2-8% CaO	H_3PO_4 = 30 *m*	30.15 ± 0.39
P152	28	60% $La(OH)_3$-32% UO_2-8% CaO	H_3PO_4 = 30 *m*	30.14 ± 0.41
P155	19	80% $La(OH)_3$-16% UO_2-4% CaO	H_3PO_4 = 30 *m*	30.03 ± 0.44
P156	14	60% $La(OH)_3$-32% UO_2-8% CaO	H_3PO_4 = 5 *m*	29.36 ± 0.51
P157	14	80% $La(OH)_3$-16% UO_2-4% CaO	H_3PO_4 = 5 *m*	29.99 ± 0.36
P158	14	37.5% $La(OH)_3$-50% UO_2-12.5% CaO	H_3PO_4 = 5 *m*	29.98 ± 0.43
P159	14	8.13% $La(OH)_3$-74% UO_2-17.87% CaO	H_3PO_4 = 5 *m*	29.59 ± 0.65
P206*	14	88.5% $La(OH)_3$-11.5% UO_2 + CaO	H_3PO_4 = 30 *m*	30.20 ± 0.34
P207*	14	80% $La(OH)_3$-20% UO_2 + CaO	H_3PO_4 = 30 *m*	30.25 ± 0.36
P208*	14	60% $La(OH)_3$-40% UO_2 + CaO	H_3PO_4 = 30 *m*	30.19 ± 0.41
P209*	14	41.85% $La(OH)_3$-58.15% UO_2 + CaO	H_3PO_4 = 30 *m*	30.03 ± 0.87
P210*	14	78% UO_2-22% CaO	H_3PO_4 = 30 *m*	29.41 ± 0.46
P213	14	88.5% $La(OH)_3$-11.5% UO_2 + CaO	H_3PO_4 = 30 *m*	30.31 ± 0.39
P214	14	79.96% $La(OH)_3$-20.04% UO_2 + CaO	H_3PO_4 = 30 *m*	30.19 ± 0.42
P215	14	60% $La(OH)_3$-40% UO_2 + CaO	H_3PO_4 = 30 *m*	29.68 ± 0.47
P216	14	41.85% $La(OH)_3$-58.15% UO_2 + CaO	H_3PO_4 = 30 *m*	29.66 ± 0.78
P217	14	78% UO_2-22% CaO	H_3PO_4 = 30 *m*	29.20 ± 0.25

Note: All experiments were performed at 780 °C, 200 MPa, pH < 0.
* Experiments with a large temperature gradient between the two ends of the gold capsule (75 °C).

gel to produce mixtures with the stoichiometries $La_2O_3 \cdot x(CaO, UO_{2.12})$ with seven different x values ranging from 0 to 0.5. The mixtures were then homogenized by grinding in an agate mortar.

The double-capsule technique was used for the hydrothermal syntheses. A mixture of 300 mg Ni + NiO and 100 mg of H_2O was loaded into a platinum capsule (30 mm long, 3.6 mm diameter, 0.1 mm thick wall) sealed by welding. An outer gold capsule (60 mm long, 5 mm diameter, 0.1 mm thick wall) enclosing the platinum capsule contained the initial reactants, which included 200 mg of orthophosphoric acid (30 *m*) and 150 mg of solids. The gold capsule was then welded shut. Preexperimental rupture tests were systematically made by heating the gold capsules overnight in an oven at 120 °C, followed by weighing to check for leaks.

Experimental methods

The experiments were conducted at 780 ± 15 °C and 200 ± 10 MPa, using cold-seal vessels (Frantz and Popp, 1979). Both conventional and rapid quench autoclaves (5 min and 1–2 s, respectively) were used. The temperatures were measured with calibrated Ni-NiCr thermocouples in an external borehole of the autoclave. The temperature gradient between the two ends of gold capsule (60 mm long, 5.8 mm o.d.) was approximately 15 °C. A mixture of water and water-soluble oil was used as a pressure medium, and the total pressure was measured using a Heise gauge.

ANALYTICAL METHODS

Characterization of samples

After quenching to room temperature and atmospheric pressure, the gold capsule was opened, and the solid phase was extracted, washed with water, and dried. The buffer was checked by X-ray diffractometry to determine whether any of the phases had been exhausted during the experiment. The products were analyzed by X-ray diffractometry, electron microprobe, and transmission electron microprobe.

X-ray diffractometry

Powder X-ray diffraction data were collected at 25 °C using Cu$K\alpha$ radiation (λ = 1.5405 Å). This technique yielded a peak resolution with an uncertainty of ±0.005 Å. The zero 2θ angle was checked after each diffractogram. The diffractometer was standardized two times a week with a quartz external standard. The difference between the theoretical and real values of the diffraction angle was within 0.05°. Diffraction lines were indexed by comparison with the JCP-DS charts. Observed values of d were indexed on the basis of a primitive monoclinic unit cell. The cell-parameter values were refined using crystallographic computer programs.

Electron microprobe analysis

A quantitative determination of the composition of the solid phases was conducted on polished grain mounts using a CAMECA SX50 electron microprobe. An acceleration voltage of 15 keV, a 10 nA beam current, and a short integration period (10 s) were used. The diameter of the electron beam was 1 μm. Standards used for the calibration were as follows: La$L\alpha$ from synthetic $(La_{0.221}Ce_{0.461}Pr_{0.044}Nd_{0.230}Sm_{0.020}Gd_{0.020})PO_4$ (Montel et al., 1989); P$K\alpha$ from synthetic $(La_{0.221}Ce_{0.461}Pr_{0.044}Nd_{0.230}Sm_{0.020}Gd_{0.020})PO_4$; U$M\alpha$ from sintered $UO_{2.12}$; and Ca$K\alpha$ from synthetic $CaSiO_3$. O contents were calculated by stoichiometry. Crystals obtained from experiments less than two weeks in duration were smaller than the diam-

TABLE 1.—*Continued*

Expt.	CaO (wt%)	La_2O_3 (wt%)	UO_2 (wt%)	Total (wt%)	O (at%)	P (at%)	La (at%)	Ca (at%)	U (at%)
P145	12.70 ± 0.27	0.03 ± 0.08	57.15 ± 0.65	100.89 ± 0.76	66.48	16.50	0.01	8.80	8.22
P146	6.07 ± 0.45	34.49 ± 2.15	29.24 ± 1.70	96.12 ± 4.17	66.65	16.62	8.27	4.23	4.23
P147	6.17 ± 0.75	33.84 ± 4.06	30.23 ± 3.45	95.79 ± 3.77	66.61	16.49	8.17	4.33	4.40
P148	5.56 ± 0.46	38.52 ± 2.40	27.19 ± 1.91	94.91 ± 6.66	66.47	16.14	9.43	3.95	4.02
P149	5.74 ± 0.18	37.67 ± 0.84	27.40 ± 0.88	97.93 ± 5.39	66.50	16.28	9.15	4.05	4.02
P150	5.63 ± 0.28	37.90 ± 1.50	27.16 ± 1.41	99.54 ± 2.22	66.53	16.32	9.20	3.97	3.98
P151	5.92 ± 0.45	35.47 ± 2.29	28.45 ± 1.83	98.89 ± 2.55	66.64	16.62	8.51	4.12	4.12
P152	5.71 ± 0.32	36.45 ± 2.04	27.68 ± 1.74	98.56 ± 1.25	66.65	16.62	8.75	3.98	4.01
P155	2.79 ± 0.45	53.47 ± 2.97	13.70 ± 2.45	98.09 ± 0.62	66.63	16.59	12.85	1.95	1.99
P156	6.44 ± 0.53	31.46 ± 3.11	32.74 ± 2.42	99.87 ± 1.75	66.61	16.39	7.62	4.57	4.82
P157	3.12 ± 0.55	49.64 ± 3.52	17.25 ± 3.01	99.78 ± 0.92	66.71	16.61	11.98	2.19	2.51
P158	9.51 ± 0.33	15.33 ± 1.19	45.18 ± 0.85	101.13 ± 0.69	66.60	16.53	3.68	6.64	6.55
P159	12.11 ± 0.26	1.99 ± 2.08	56.30 ± 1.53	101.74 ± 1.57	66.49	16.36	0.48	8.48	8.19
P206*	1.27 ± 0.14	62.38 ± 0.76	6.15 ± 0.64	99.70 ± 0.42	66.65	16.62	14.96	0.88	0.89
P207*	2.89 ± 0.16	52.60 ± 0.92	14.26 ± 0.92	98.19 ± 1.70	66.67	16.64	12.61	2.01	2.06
P208*	5.08 ± 0.36	40.59 ± 1.82	24.14 ± 1.34	99.98 ± 0.45	66.64	16.61	9.73	3.54	3.49
P209*	4.73 ± 0.35	42.59 ± 1.62	22.66 ± 1.61	99.77 ± 0.85	66.62	16.56	10.23	3.30	3.29
P210*	12.66 ± 0.17	0.00 ± 0.00	57.93 ± 0.62	102.35 ± 1.95	66.42	16.28	0.00	8.87	8.43
P213	1.44 ± 0.21	61.11 ± 1.41	7.15 ± 0.99	98.25 ± 0.82	66.67	16.66	14.64	1.00	1.03
P214	3.22 ± 0.60	50.61 ± 3.33	15.97 ± 2.91	98.76 ± 1.53	66.67	16.63	12.14	2.25	2.31
P215	5.67 ± 0.58	37.55 ± 3.18	27.11 ± 2.54	99.87 ± 1.38	66.57	16.44	9.06	3.98	3.95
P216	8.19 ± 0.41	23.32 ± 1.40	38.83 ± 2.12	98.62 ± 2.81	66.55	16.42	5.63	5.74	5.65
P217	12.71 ± 0.24	0.00 ± 0.00	58.09 ± 0.10	103.44 ± 0.61	66.39	16.21	0.00	8.93	8.48

eter of the electron beam. In this case, the analyses of the crystal compositions led to more dispersed results (Table 1).

Transmission electron microprobe

The TEM investigations were performed with a PHILIPS CM 20 instrument using 200 kV accelerating voltage. Element analyses were performed through the thinnest particles by energy-dispersive spectroscopy, using an EDAX spectrometer equipped with a Be super-thin window. A synthetic monazite of known composition was used as an external standard. The elements analyzed were P$K\alpha$, La$L\alpha$, Ca$K\alpha$, and U$M\alpha$.

RESULTS

Equilibrium conditions in the system

Crystals of monazite with seven compositions of U and Ca were synthesized. The experiments yielded small but well-crystallized green monazite crystals ranging in size from 0.2 to 20 μm (Fig. 1) and crystals of UP_2O_7, which always coprecipitate with U- and Ca-bearing monazite. Their origin can be attributed to an excess of U in comparison with the Ca content in the initial mixture. Results obtained from electron microprobe analyses (Table 1) show that the compositions of monazite were homogeneous after each experiment. The TEM investigations showed that the compounds synthesized are homogeneous at the scale of 10^5 nm^3. The variations of the distribution of U and Ca in monazite are <5% (relative). No precipitates were observed in the crystals.

A kinetic study was performed to determine the minimum experiment duration required to reach equilibrium. The results obtained (Fig. 2) indicate that after 1 d monazite had crystallized and incorporated all the available U and Ca. For initial mixtures of similar composition, 1-day and 1-month experiments resulted in monazite crystals with similar composition. The average crystal size increased from 0.2 to 10 μm, with increasing duration from 1 to 50 d. Only experiments of more than two weeks duration produced monazite crystals large enough ($\geq$2 μm) to be analyzed by electron microprobe.

Four experiments were conducted by maintaining a large temperature gradient (approximately 75 °C) be-

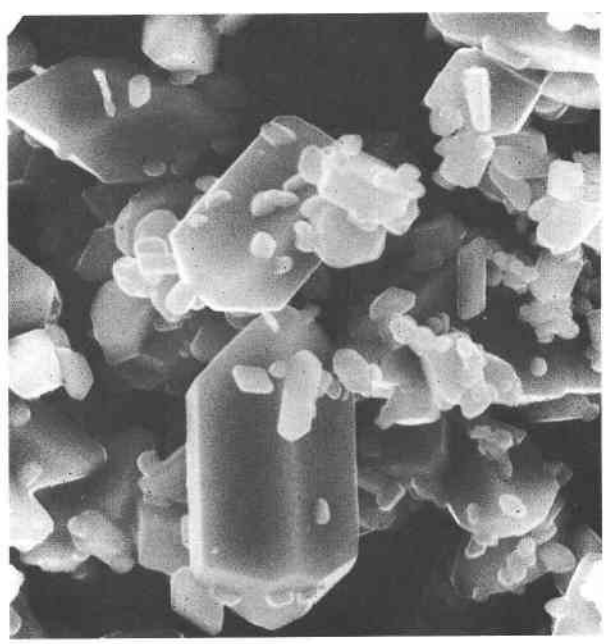

Fig. 1. SEM photomicrograph of crystals of $(La_{0.5}U_{0.25}Ca_{0.25})PO_4$ synthesized in 30 *m* H_3PO_4, at 780 °C, 200 MPa, and under reducing conditions (Ni + NiO buffer).

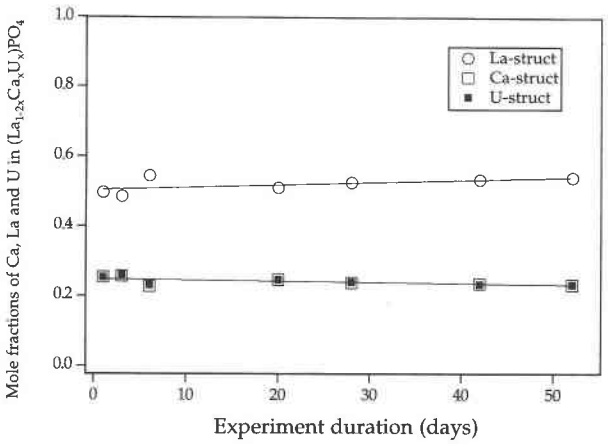

Fig. 2. Substitution of U and Ca in $(La_{0.5}U_{0.25}Ca_{0.25})PO_4$ vs. experiment duration.

tween the two ends of the gold capsule. This experimental condition led to the formation of gem-quality acicular crystals of U- and Ca-bearing monazite up to 200 μm long.

The solubility of monazite containing U and Ca in H_3PO_4 = 30 *m* could not be measured because this solid phase always coexisted with UP_2O_7 crystals.

Mechanism of U and Ca substitution in $LaPO_4$

A good one-to-one relationship between U and Ca (in atomic percent) in the monazite synthesized in the present study shows that the same number of U and Ca atoms was incorporated into the structure of $LaPO_4$ (Fig. 3a). A linear correlation was also obtained between La and U + Ca (in atomic percent) (Fig. 3b). These correlations between U, Ca, and La in monazite at the f_{O_2} value fixed by the Ni + NiO buffer (Chou, 1978; Calas, 1979; Peiffert et al., 1994) show that U in the monazite can only be tetravalent. Furthermore, Kelly et al. (1981) determined by optical absorption spectrophotometry that the valence state of U in synthetic monazite is primarily tetravalent. Thus, charge compensation for the $U^{4+} \rightleftharpoons La^{3+}$ substitution is realized by a $Ca^{2+} \rightleftharpoons La^{3+}$ substitution. This type of charge-compensation mechanism is analogous to that proposed by Bowie and Horne (1953) and Frondel (1948) to explain the Ca + Th substitution in monazite. The substitution reaction can be written as

$$LaPO_4 + xU^{4+} + xCa^{2+} = (La_{1-2x}U_xCa_x)PO_4 + 2xLa^{3+}. \quad (3)$$

The mole fraction x is defined by the ratio

$$x = U/(La + Ca + U) \quad (4)$$

where the concentration of each element is expressed in atomic percent.

This type of substitution mechanism was proposed by Brouand and Cuney (1990). These authors performed a mono- and multivariable statistical study of more than 500 electron microprobe analyses of monazite. They

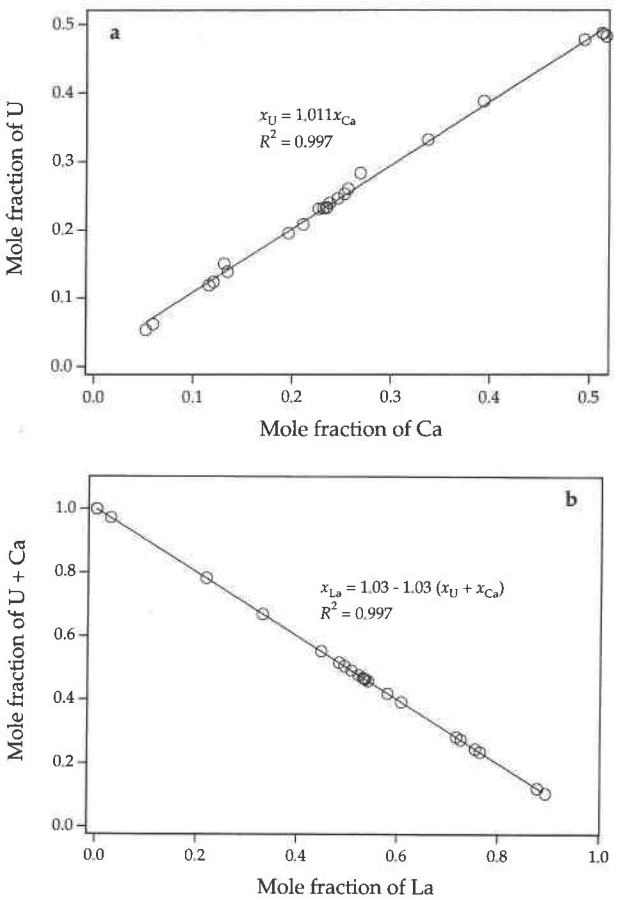

Fig. 3. (a) Linear correlation between mole fractions of U and those of Ca in synthetic $(La_{1-2x}U_xCa_x)PO_4$ solid solution. (b) Linear correlation between mole fractions of U and Ca and those of La in synthetic $(La_{1-2x}U_xCa_x)PO_4$ solid solution. R = correlation coefficient.

showed that a coupled substitution of U and Th with Ca allows a large substitution of radioelements in monazite.

Synthesis of the compound $(Ca_{0.5}U_{0.5})PO_4$

The end-member $(Ca_{0.5}U_{0.5})PO_4$ was hydrothermally synthesized from a homogeneous stoichiometric mixture of $UO_{2.12}$ and CaO in H_3PO_4 = 30 *m*. At T = 780 °C, P = 200 MPa, and f_{O_2} buffered by Ni + NiO, $(Ca_{0.5}U_{0.5})PO_4$ is stable in the range 5–30 *m* H_3PO_4. The compound $(Ca_{0.5}U_{0.5})PO_4$ does not form in $H_3PO_4 \leq 1$ *m*, and in a H_3PO_4-KH_2PO_4 solution, pH = 2.2 (T = 780 °C, P = 200 MPa).

The composition of the compound $(Ca_{0.5}U_{0.5})PO_4$ was determined by electron microprobe analysis. The analyses always yielded an excess value of Ca^{2+} in the compound formula, and the total oxide weight determined was always higher than 100. TEM photomicrographs do not show the presence of Ca-bearing microphases in the structure at the nanometer level.

The size of the crystals is in the range of 5–10 μm. The crystals were obtained by maintaining a temperature gra-

TABLE 2. Crystallographic data for $(Ca_{0.5}U_{0.5})PO_4$

d_{obs}* (Å)	d_{obs}** (Å)	d_{calc}† (Å)	*hkl*	*hkl*
5.14	4.96	5.122	$\bar{1}01$	
4.70	4.76	4.695	110	
4.58	4.57	4.581	011	
4.11	4.09	4.098	$\bar{1}11$	
4.03	4.00	4.002	101	
3.42	3.400	3.416	020	
3.24	3.222	3.225	200	
3.03	3.025	3.018	120	
2.919	2.919	2.915	210	
2.817	2.811	2.807	012	$\bar{1}12$
2.564	2.561	2.555	$\bar{2}02$	
2.402	2.395	2.386	112	$\bar{2}12$
2.350	2.349	2.342	220	
2.208	2.204	2.197	$\bar{3}01$	
2.142	2.139	2.131	031	
2.102	2.113	2.105	$\bar{1}03$	
2.077	2.074	2.068	221	
1.920	1.921	1.912	212	
1.893	1.896	1.886	301	
1.860	1.857	1.846	$\bar{2}31$	
1.836	1.836	1.826	103	
1.822	1.822	1.812	320	
1.758	1.763	1.752	023	
1.736	1.732	1.721	$\bar{3}22$	
1.703	1.702	1.691	132	$\bar{2}32$

* From $(Ca_{0.5}U_{0.5})PO_4$ synthesized in 30 *m* H_3PO_4 at T = 780 °C, P = 200 MPa.
** From $(Ca_{0.5}U_{0.5})PO_4$ heated at 1200 °C in air for 2 h.
† Refined using crystallographic computer programs.

dient of approximately 75 °C between the two ends of the gold capsule. X-ray data obtained from powder patterns showed that this compound is isostructural with high-temperature monoclinic monazite (see Table 2). Cell parameters were calculated from the value of the identified peaks. The lattice constants are a_0 = 6.654(6), b_0 = 6.840(8), c_0 = 6.359(6) Å, and β_0 = 103.98(11)°.

The crystals were heated at 1200 °C for 2 h in air. The compound did not decompose or oxidize, as described by Muto et al. (1959). Rather, small crystals agglomerated to form larger crystals. The composition of these crystals is always $(Ca_{0.5}U_{0.5})PO_4$. The values of the X-ray powder peaks are similar to those reported in Table 2. The crystals crystallized in the monoclinic structure.

The $LaPO_4$-$(Ca_{0.5}U_{0.5})PO_4$ solid solution

X-ray data for the synthesized solid phases are similar to high-temperature monazite X-ray data (Pepin and Vance, 1981). Refined unit-cell parameters for $(La_{1-2x}U_xCa_x)PO_4$ were calculated for values of the mole fraction x from the peak values unequivocally identified. The results are presented in Table 3, along with data for natural monazite. Unit-cell constants and unit-cell volumes are plotted against the mole fraction x of U and Ca in $LaPO_4$ (Fig. 4a–4c). The plots show that the unit-cell parameters decrease linearly with the increase of the U-Ca substitution in $LaPO_4$. This decrease results from increasing substitution of elements (U^{4+} and Ca) with smaller ionic radii. The ionic radii of U^{4+}, Ca^{2+}, and La^{3+} are 1.05, 1.18, and 1.216 Å, respectively (Shannon, 1976). These results show that a complete solid solution exists between the two end-members $LaPO_4$ and $(Ca_{0.5}U_{0.5})PO_4$ at 780 °C, 200 MPa, 30 *m* H_3PO_4, and f_{O_2} buffered by Ni + NiO.

DISCUSSION

In the intermediate compounds $(La_{1-2x}U_xCa_x)PO_4$, $2xLa^{3+}$ cations are replaced in the monazite unit cell by

TABLE 3. Data for the unit-cell constants of $(La_{1-2x}U_xCa_x)PO_4$

Expt.	Compound	x	a_0 (Å)	b_0 (Å)	c_0 (Å)	β_0 (°)	V_0 (Å³)	Reference
	$LaPO_4$	0.000	6.790	7.040	6.470	104.400	299.000	Bowie and Horne, 1953
	$LaPO_4$	0.000	6.837	7.077	6.510	103.240	306.500	Pepin and Vance, 1981
	$LaPO_4$	0.000	6.825	7.057	6.482	103.210	303.900	Mullica et al., 1984
	$LaPO_4$	0.000	6.682	7.044	6.539	104.250	307.200	Montel et al., 1989
P20	$LaPO_4$	0.000	6.824	7.056	6.495	103.310	304.343	this work
P60	$LaPO_4$	0.000	6.822	7.070	6.486	103.278	304.441	this work
P61	$LaPO_4$	0.000	6.819	7.061	6.486	103.267	303.938	this work
P62	$LaPO_4$	0.000	6.819	7.057	6.496	103.295	304.181	this work
P63	$LaPO_4$	0.000	6.815	7.057	6.497	103.252	304.172	this work
P206	$(La_{0.894}U_{0.053}Ca_{0.053})PO_4$	0.053	6.823	7.057	6.498	103.316	304.441	this work
P213	$(La_{0.870}U_{0.065}Ca_{0.065})PO_4$	0.065	6.830	7.064	6.491	103.375	304.637	this work
	$(REE_{0.800}U_{0.100}Ca_{0.100})PO_4$	0.100	6.725	6.938	6.415	103.700	290.800	McCarthy et al., 1978
P207	$(La_{0.755}U_{0.123}Ca_{0.120})PO_4$	0.122	6.811	7.049	6.479	103.411	302.561	this work
P214	$(La_{0.727}U_{0.138}Ca_{0.135})PO_4$	0.136	6.790	7.015	6.476	103.424	300.035	this work
P157	$(La_{0.644}U_{0.128}Ca_{0.128})PO_4$	0.128	6.756	7.004	6.440	103.446	296.354	this work
	$(REE_{0.600}U_{0.200}Ca_{0.200})PO_4$	0.200	6.716	6.925	6.408	103.760	289.500	McCarthy et al., 1978
P208	$(La_{0.581}U_{0.208}Ca_{0.211})PO_4$	0.210	6.766	6.982	6.446	103.598	295.974	this work
P148	$(La_{0.546}U_{0.227}Ca_{0.227})PO_4$	0.227	6.742	6.955	6.431	103.664	293.029	this work
P150	$(La_{0.538}U_{0.231}Ca_{0.231})PO_4$	0.231	6.733	6.951	6.432	103.614	292.547	this work
P215	$(La_{0.533}U_{0.234}Ca_{0.233})PO_4$	0.234	6.757	6.966	6.456	103.690	295.240	this work
P149	$(La_{0.532}U_{0.234}Ca_{0.234})PO_4$	0.234	6.733	6.958	6.420	103.565	292.383	this work
P147	$(La_{0.488}U_{0.256}Ca_{0.256})PO_4$	0.256	6.734	6.947	6.430	103.603	292.388	this work
P146	$(La_{0.484}U_{0.258}Ca_{0.258})PO_4$	0.258	6.732	6.948	6.432	103.720	292.240	this work
P156	$(La_{0.456}U_{0.272}Ca_{0.272})PO_4$	0.272	6.718	6.948	6.426	103.723	291.374	this work
P216	$(La_{0.331}U_{0.332}Ca_{0.337})PO_4$	0.333	6.725	6.939	6.422	103.879	290.925	this work
P158	$(La_{0.206}U_{0.397}Ca_{0.397})PO_4$	0.397	6.688	6.883	6.380	104.073	284.828	this work
P210	$(U_{0.487}Ca_{0.513})PO_4$	0.500	6.661	6.851	6.360	104.134	281.438	this work
P212	$(Ca_{0.5}U_{0.5})PO_4$	0.500	6.673	6.852	6.364	104.068	282.274	this work
P145	$(Ca_{0.5}U_{0.5})PO_4$	0.500	6.653	6.845	6.356	104.025	280.797	this work

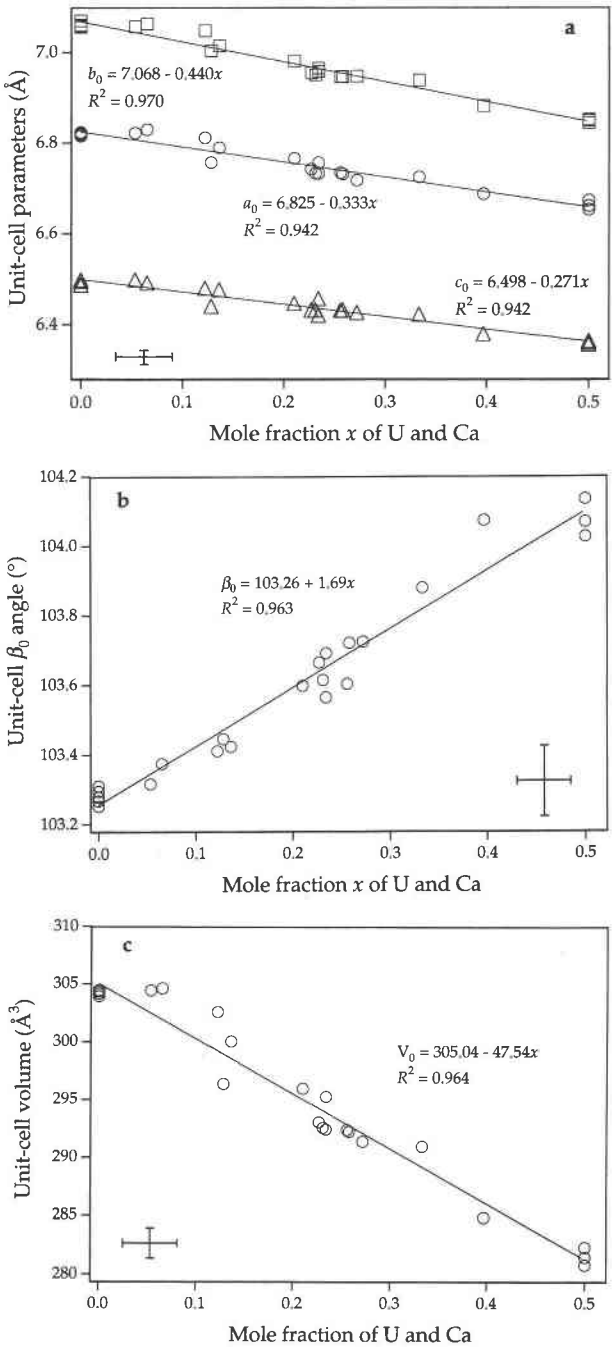

Fig. 4. (**a**) Linear correlation between unit-cell parameters (a_0, b_0, c_0) (Å) of synthetic $(La_{1-2x}U_xCa_x)PO_4$ solid solution and mole fraction x of U and Ca. The cross in the lower left corner of the diagram gives the maximum error in the unit-cell parameters and the maximum 1σ in the mole fraction data. Open circles = a_0, open squares = b_0, open triangles = c_0. (**b**) Linear correlation between unit-cell angle β_0 of synthetic $(La_{1-2x}U_xCa_x)PO_4$ solid solution and mole fraction x of U and Ca. The cross in the lower right corner of the diagram gives the maximum error in the unit-cell angle and the maximum 1σ in the mole fraction data. (**c**) Variations of unit-cell volume, V_0, of synthetic $(La_{1-2x}U_xCa_x)PO_4$ solid solution vs. mole fractions of U and Ca. The cross in the lower left corner of the diagram gives the maximum error in the unit-cell volume and the maximum 1σ in the mole fraction data.

xU^{4+} and xCa^{2+} cations. The average cation site contains $(1 - 2x)La^{3+}$ ion, xU^{4+} ion, and xCa^{2+} ion. The average ionic radius of the cation site in $(La_{1-2x}U_xCa_x)PO_4$ is expressed by the equation

$$^{[9]}r_{Cat^{3+}} = (1 - 2x)\,^{[9]}r_{La^{3+}} + x\,^{[9]}r_{U^{4+}} + x\,^{[9]}r_{Ca^{2+}} \quad (5)$$

Where $^{[9]}r_{La^{3+}}$, $^{[9]}r_{U^{4+}}$, and $^{[9]}r_{Ca^{2+}}$ are the ionic radii of La^{3+}, U^{4+}, and Ca^{2+}, respectively, in the ninefold coordination (from Shannon, 1976).

The experimental values of the unit-cell parameters of synthesized $(La_{1-2x}U_xCa_x)PO_4$ compounds were plotted in Figure 5a and 5b vs. the average ionic radius of the cation site. The following linear correlations were established:

$$a_0 = 1.652\,^{[9]}r_{Cat^{3+}} + 4.816 \quad (6)$$

$$b_0 = 2.182\,^{[9]}r_{Cat^{3+}} + 4.414 \quad (7)$$

$$c_0 = 1.342\,^{[9]}r_{Cat^{3+}} + 4.866 \quad (8)$$

$$\beta_0 = -8.353\,^{[9]}r_{Cat^{3+}} + 113.41. \quad (9)$$

The Correlations 6, 7, 8, and 9 show that the decrease of the unit-cell constants results from the contraction of the cation site in the $LaPO_4$ structure. Similar equations can be established from the relationship between the unit-cell parameters (Pepin and Vance, 1981; Beall et al., 1981; Mullica et al., 1984, 1985a, 1985b) of $REEPO_4$ and the ionic radii of the REE^{3+} cations:

$$a_0 = 1.773\,^{[9]}r_{REE^{3+}} + 4.674 \quad (10)$$

$$b_0 = 2.135\,^{[9]}r_{REE^{3+}} + 4.466 \quad (11)$$

$$c_0 = 1.612\,^{[9]}r_{REE^{3+}} + 4.534 \quad (12)$$

$$\beta_0 = -7.069\,^{[9]}r_{REE^{3+}} + 111.91. \quad (13)$$

A comparison of Equations 6, 7, 8, and 9 with Equations 10, 11, 12, and 13 shows that the rates of contraction of the three unit-cell parameters a_0, b_0, and c_0 are comparable in the $(La_{1-2x}U_xCa_x)PO_4$ solid solution and in the $REEPO_4$ series. The coupled substitution of U and Ca cations in monazite does not distort the unit cell of $(La_{1-2x}U_xCa_x)PO_4$. Thus, it can be concluded that the atoms of U and Ca incorporated in monazite do not present any specific ordering. The ability of $LaPO_4$ to accommodate extensive U-Ca substitution may be due to the irregular coordination existing around La^{3+} ions, which does not place severe symmetry constraints on the cations (Beall et al., 1981). The study of the structure of $(Ca_{0.5}U_{0.5})PO_4$ should provide the exact position of the atoms in the unit cell as well as information relative to the cation site occupation in $(La_{1-2x}U_xCa_x)PO_4$ compounds.

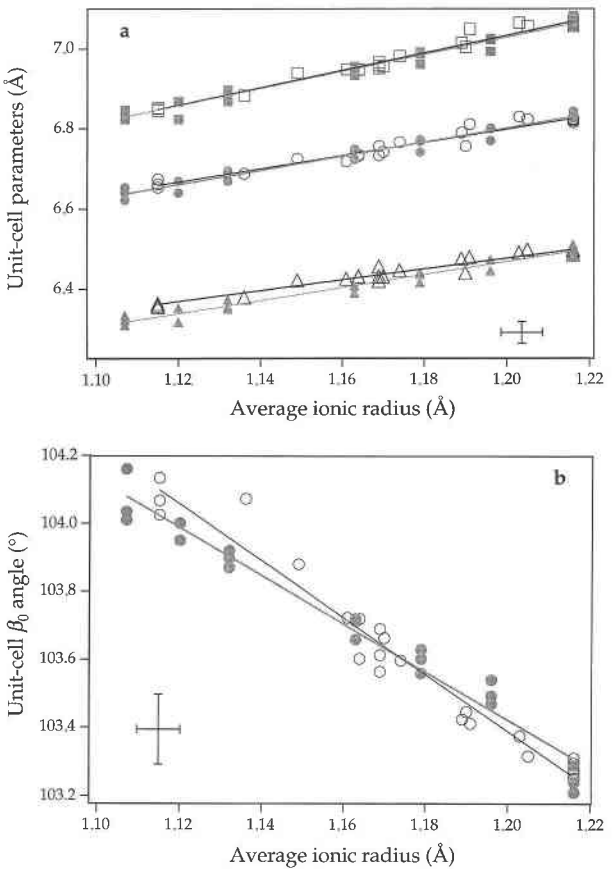

Fig. 5. (a) Unit-cell parameters plotted as a function of the ionic radii of REE^{3+} in $REEPO_4$ and the average ionic radii of the cation site in $(La_{1-2x}U_xCa_x)PO_4$. The cross in the lower right corner of the diagram gives the maximum error in the unit-cell parameters and the maximum 1σ in the ionic radii data. Open circles = a_0, open squares = b_0, and open triangles = c_0 of $(La_{1-2x}U_xCa_x)PO_4$. Shaded circles = a_0, shaded squares = b_0, and shaded triangles = c_0 of $REEPO_4$. (b) Unit-cell angles plotted as a function of the ionic radii of REE^{3+} in $REEPO_4$ and the average ionic radii of the cation site in $(La_{1-2x}U_xCa_x)PO_4$. The cross in the lower left corner of the diagram gives the maximum error in the unit-cell angle and the maximum 1σ in the ionic radii data. Open circles = β_0 of $(La_{1-2x}U_xCa_x)PO_4$, shaded circles = β_0 of $REEPO_4$.

Geological and environmental implications

The experimental results show that there is no crystal-chemical limitation to the substitution of U in monazite under pressure and temperature conditions corresponding to those of granitic magmas, provided that reducing conditions are available to maintain U in the tetravalent state. The limitations to coupled U-Ca substitution mainly result from the low amounts of U contained in these magmas and the melt-monazite partition coefficients of U.

Monazite was proposed (McCarthy et al., 1978; Boatner and Beall, 1978; Boatner and Sales, 1988, for example) as an ideal host for the actinides contained in nuclear wastes. The complete solid solution between $LaPO_4$ and $(Ca_{0.5}U_{0.5})PO_4$ is proof of the large capacity of monazite to incorporate U. Further work is necessary to determine the most stable composition of $(La_{1-2x}U_xCa_x)PO_4$ in different systems.

Acknowledgments

The high-pressure and high-temperature experiments were performed in the Experimental Laboratory of the Centre de Recherches Pétrographiques et Géochimiques (CRPG), France. The authors thank A. Rouillier, F. Lhote (CRPG), J. Ghanbaja, J.M. Claude, and A. Khöler (Université de Nancy I) for their technical and analytical support. Critical reviews by L.A. Boatner and an anonymous reviewer greatly improved this manuscript.

References cited

Anthony, J.W. (1957) Hydrothermal synthesis of monazite. American Mineralogist, 42, 904.

——— (1965) Crystal morphology of thorium-bearing synthetic monazite. American Mineralogist, 50, 1421–1431.

Beall, G.W., Boatner, L.A., Mullica, D.F., and Milligan, W.O. (1981) The structure of cerium orthophosphate, a synthetic analogue of monazite. Journal of Inorganic and Nuclear Chemistry, 43, 101–105.

Boatner, L.A., and Beall, G.W. (1978) Letter to the U.S. Department of Energy on 28 April 1978, detailing possible uses of monazite as an alternative to borosilicate glass. Personal communication. Cited in Boatner and Sales (1988).

Boatner, L.A., and Sales, B.C. (1988) Radioactive waste forms for the future: Monazite. In W. Lutze and R.C. Ewing, Eds., Radioactive waste forms for the future, p. 495–564. North-Holland, Amsterdam.

Bowie, S.H.U., and Horne, J.E.T. (1953) Cheralite, a new mineral of the monazite group. Mineralogical Magazine, 30, 93–99.

Brouand, M., and Cuney, M. (1990) Substitution des radioéléments dans la monazite des granites hyperalumineux: Conséquences pour la définition de leur potentialité métallogénique. Bulletin de la Société française de Minéralogie et de Cristallographie, 2/3, 124–125.

Calas, G. (1979) Etude expérimentale du comportement de l'uranium dans les magmas, états d'oxydation et de coordinence. Geochimica and Cosmochimica Acta, 43, 1521–1531.

Chou, I-M. (1978) Calibration of oxygen buffers at elevated *P* and *T* using the hydrogen fugacity sensor. American Mineralogist, 63, 690–703.

Frantz, J.D., and Popp, R.K. (1979) Mineral-solution equilibria: I. An experimental study of complexing and thermodynamic properties of aqueous $MgCl_2$ in the system MgO-SiO_2-H_2O-HCl. Geochimica et Cosmochimica Acta, 43, 1223–1239.

Frondel, C. (1948) Systematic mineralogy of uranium and thorium. U.S. Geological Survey Bulletin, 1064, 151–152.

Gramaccioli, C.M., and Segalstad, T.V. (1978) A uranium- and thorium-rich monazite from a south-alpine pegmatite at Piona, Italy. American Mineralogist, 63, 757–761.

Karkhanavala, M.D. (1956) The synthesis of huttonite and monazite. Current Science, 5, 166–167.

Kelly, K.L., Beall, G.W., Young, J.P., and Boatner, L.A. (1981) Valence states of actinides in synthetic monazites. In Scientific Basis for Nuclear Waste Management, 3, 189–195.

McCarthy, G.J., White, W.B., and Pfoertsch, D.E. (1978) Synthesis of nuclear waste monazite, ideal actinide hosts for geological disposal. Material Research Bulletin, 13, 1239–1245.

Montel, J.M., Lhote, F., and Claude, J.M. (1989) Monazite end-members and solid solutions: Synthesis, unit-cell characteristics and utilization as microprobe standards. Mineralogical Magazine, 53, 120–123.

Mooney, R.C.L. (1948) Crystal structures of a series of rare-earth phosphates. Journal of Chemical Physics, 16, 1003.

Mullica, D.F., Milligan, W.O., Grossie, D.A., Beall, G.W., and Boatner, L.A. (1984) Ninefold coordination in $LaPO_4$: Pentagonal interpenetrating tetrahedral polyhedron. Inorganica Chimica Acta, 95, 231–236.

Mullica, D.F., Grossie, D.A., and Boatner, L.A. (1985a) Coordination geometry and structural determinations of samarium orthophosphate, europium orthophosphate and gadolinium orthophosphate. Inorganica Chimica Acta, 109(2), 105–110.

——— (1985b) Structural refinements of praseodinium orthophosphate

and neodinium orthophosphate. Journal of Solid State Chemistry, 58(1), 71–77.

Muto, T., Meyrowitz, R., Pommer, A.M., and Murano, T. (1959) Ningyoite, a new uranous phosphate mineral from Japan. American Mineralogist, 44, 633–650.

Overstreet, W.C. (1967) The geologic occurrence of monazite. U.S. Geological Survey Professional Paper, 530, 327 p.

Peiffert, C., Cuney, M., and Nguyen-Trung, C. (1994) Uranium in granitic magmas: 1. Experimental determination of uranium solubility and fluid melt. Partition coefficient in the uranium oxide-haplogranite-H_2O-Na_2CO_3 system at 720–770°C, 2 kbar. Geochimica and Cosmochimica Acta, 58(11), 2495–2507.

Pepin, G.J., and Vance, E.R. (1981) Crystal data for rare earth orthophosphates of the monazite structure-type. Journal of Inorganic and Nuclear Chemistry, 43(11), 2807–2809.

Pepin, G.J., Davis, D.D., McCarthy, G.J., and Vance, E.R. (1981) Crystal chemistry of some monazite-structured phosphates and silicates. DOE/ET/41 900-7, ESG-EOG-13 351, 37 p.

Radominski, M.F. (1875) Reproduction artificielle de la monazite et de la xénotime. Comptes Rendus de l'Académie des Sciences de Paris, 80, 304–307.

Shannon, R.D. (1976) Revised effective ionic radii and systematic studies of interatomic distances in halides and chalcogenides. Acta Crystallographica, A32, 751–767.

Manuscript received September 14, 1994
Manuscript accepted July 7, 1995